# TWO-POWER-LAW RELAXATION PROCESSES IN COMPLEX MATERIALS*

Agnieszka Jurlewicz

Hugo Steinhaus Center, Institute of Mathematics and Computer Science
Wrocław University of Technology
Wyb. Wyspiańskiego 27, 50-370 Wrocław, Poland

Justyna Trzmiel, Karina Weron

Institute of Physics, Wrocław University of Technology
Wyb. Wyspiańskiego 27, 50–370 Wrocław, Poland

*(Received January 25, 2010)*

We show that a turnover from the classical Debye to the two-power-law relaxation behavior, observed in the majority of physical systems, is associated with a new type of a coupled memory continuous-time random walk driving a fractional dynamics. We derive a general class of the two-power-law relaxation responses which is able to reproduce all of the observed relaxation patterns, given by the low- and high-frequency power-law exponents falling in the range (0,1].

PACS numbers: 89.75.Kd, 02.50.Fz

## 1. Introduction

Dielectric spectroscopy investigations of different physical systems (*i.e.* polymers, alcohols, disordered crystals, amorphous and crystalline semiconductors) revealed that a wide-class of various materials exhibits a non-exponential, two-power-law relaxation pattern. The dielectric response of such systems [1] is represented by low- and high-frequency power-law dependency of the complex dielectric permittivity $\varepsilon(\omega) = \varepsilon'(\omega) - i\varepsilon''(\omega)$ on frequency:

$$\begin{aligned} \varepsilon(0) - \varepsilon'(\omega) \ &\sim \ \varepsilon''(\omega) \sim \left(\frac{\omega}{\omega_p}\right)^m, \quad \omega \ll \omega_p\,, \\ \varepsilon'(\omega) \ &\sim \ \varepsilon''(\omega) \sim \left(\frac{\omega}{\omega_p}\right)^{n-1}, \quad \omega \gg \omega_p\,, \end{aligned} \tag{1}$$

* Presented at the XXII Marian Smoluchowski Symposium on Statistical Physics, Zakopane, Poland, September 12–17, 2009.

where $\omega_p$ denotes the loss peak frequency, $\varepsilon(0)$ is the static permittivity and the power-law exponents $m$ and $n$ fall in the range of $(0,1]$. A large part of these power-law properties may be satisfactorily described by the most popular analytical expression applied to fit the frequency-domain data, *i.e.* the empirical Havriliak–Negami (HN) relaxation function:

$$\varepsilon(\omega) \sim \frac{1}{[1+(i\omega/\omega_p)^{\alpha}]^{\gamma}}\,, \quad 0<\alpha,\gamma\leq 1\,. \tag{2}$$

The power-law exponents expressed by means of the HN parameters read: $m=\alpha$, $1-n=\alpha\gamma$. For $\alpha=1$ and $\gamma<1$ formula (2) takes the form of the Cole–Davidson (CD) function, for $\alpha<1$ and $\gamma=1$ — the Cole–Cole (CC) function, whereas for $\alpha=1$ and $\gamma=1$ the Debye (D) function is obtained. It is easy to observe that the HN function fits only the relaxation data for which the power-law exponents satisfy relation $m\geq 1-n$ (see Fig. 1). Whenever the data fall in the range for which $m<1-n$, the ex-

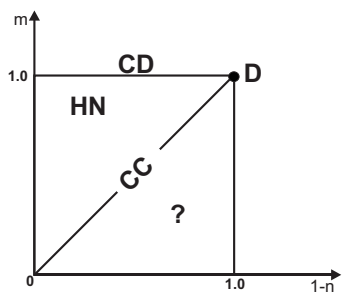


Fig. 1. Schematic representation of various cases of relaxation processes.

tended range $0<\alpha,\alpha\gamma\leq 1$ of the HN function parameters could be used [2]. Unfortunately, the theoretical approaches [3, 4] leading to the HN function fail for $\gamma>1$ and an explanation, based on simple subdiffusion mechanisms such as those involved in the CC relaxation process [5], cannot be given. To complete the diffusion scenario, underlying the two-power-law patterns, the clustered-jump continuous time random walk (CTRW), resulting from a stochastic generalization of the renormalization group transformation idea, has been proposed [6]. Implementation of this type of a CTRW allows to clarify the stochastic origins of the power-law exponents in all two-power-law empirical data. In Fig. 2 sample of the frequency-domain relaxation responses in various complex systems are presented. Both the curves exhibit single maxima peak, however, the low- and high-frequency exponents satisfy different relations discussed above. For the liquid crystalline epoxy monomer EPPEPB, which is used to fabricate polymer networks [7], the

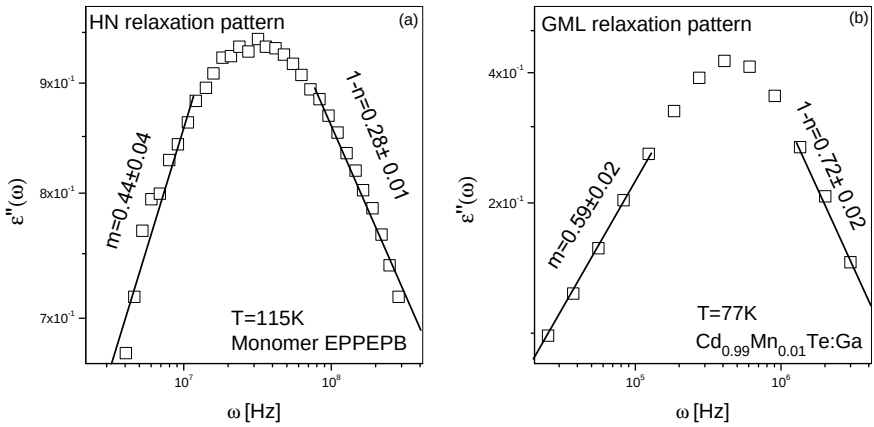


Fig. 2. Various non-exponential relaxation patterns in real systems. The HN dielectric response (a) was observed by Włodarska *et al.*, in liquid crystalline epoxy monomer EPPEPB [7]. The GML relaxation (b) was observed by us in gallium (Ga) doped semiconducting mixed crystal $Cd_{1-x}Mn_xTe$ of $x = 0.01$ manganese (Mn) content.

power-law exponents satisfy relation $m > 1 - n$, whereas for the semiconducting mixed crystal $Cd_{0.99}Mn_{0.01}Te$:Ga, used in holography or data storage [8], the power-law exponents satisfy $m < 1 - n$.

## 2. Relaxation model

Description of the dielectric relaxation phenomena by means of the complex permittivity $\varepsilon(\omega)$ is equivalent [1] to the representation utilizing notion of the time-domain relaxation function $\Phi(t)$:

$$\varepsilon(\omega) \sim \int_0^\infty \exp(-i\omega t)\left(-\frac{d\Phi(t)}{dt}\right) dt\,.$$

Then the low- and high-frequency power laws (1) correspond to the following short- and long-time power-law dependency on time:

$$-\frac{d\Phi(t)}{dt} \sim \begin{cases} (\omega_p t)^{-n} & \text{for} \quad \omega_p t \ll 1\,, \\ (\omega_p t)^{-m-1} & \text{for} \quad \omega_p t \gg 1\,. \end{cases} \tag{3}$$

The diffusion mechanism, underlying the two-power-law relaxation phenomenon, can be studied by means of the diffusion front related to the total

distance $R(t)$, reached till time $t$ by a walker performing a continuous-time random walk (CTRW) [4–6, 9–11]. The total distance $R(t)$ is equal to the sum of the walker's random jumps $R_i$:

$$R(t) = \sum_{i=1}^{\nu(t)} R_i \,, \tag{4}$$

where $\nu(t)$ denotes the random number of steps performed by the walker till time $t$ at random instants of time. The jumps $R_i$ and the inter-jump waiting times $T_i$ are assumed to form a sequence of independent and identically distributed random vectors $(R_i, T_i)$, $i \geq 1$. The diffusion front $\widetilde{R}(t)$, corresponding to (4), represents the asymptotic behavior of the rescaled total distance $f(c)R(ct)$ when dimensionless time-scale coefficient $c$ tends to $\infty$ and the space-rescaling function $f(c)$ is chosen appropriately. In this framework the temporal decay of a given mode $k$, representing excitation undergoing diffusion in the system under consideration, is represented by the inverse Fourier transform of the diffusion front: $\Phi(t) = \langle e^{-ik\widetilde{R}(t)} \rangle$. The resulting relaxation patterns are obviously connected with the stochastic properties of the jumps and the inter-jump times. Also they depend on the detailed construction of the counting process $\nu(t)$.

In the classical waiting-jump CTRW idea the jump $R_i$ occurs after the waiting-time period $T_i$. Hence, $\nu(t) = \nu_{wj}(t)$ is equal to the largest $n$ such that $\sum_{i=1}^{n} T_i \leq t$. On the other hand, if the jump-waiting CTRW scenario, in which $R_i$ precedes $T_i$, is considered, the number of jumps $\nu(t) = \nu_{jw}(t)$ is equal to the smallest $n$ such that $\sum_{i=1}^{n} T_i > t$. Both numbers of the steps performed by the walker up to time $t$ are inter-related: $\nu_{jw}(t) = \nu_{wj}(t) + 1$. In the case of the decoupled CTRW (*i.e.* when we additionally assume the stochastic independence of the jump $R_i$ and the waiting time $T_i$) these two CTRW scenarios yield exactly the same diffusion front and the corresponding type of relaxation [12]. In contrary, in the coupled cases the waiting-jump and jump-waiting schemes may lead to essentially different relaxation patterns [12].

Stochastic generalization [6] of the renormalization-group transformation idea applied to random walks [13, 14], has led to a special class of coupled, clustering-jump CTRWs with properties yielding the two-power-law relaxation patterns. The construction of the clustering-jump CTRW results originally [4, 6, 12] from assembling the jumps and inter-jump waiting times into clusters of random sizes. However, it can be defined equivalently by formula (4) with a specially constructed compound counting process $\nu(t) = \nu_{c,s}(t)$

$$\nu_{c,s}(t) = \sum_{i=1}^{\mu_s(\nu_s(t))} M_i \,, \tag{5}$$

where $s = wj$ refers to the waiting-jump scheme, $s = jw$ to the jump-waiting scheme, $\mu_{wj}(n)$ is the largest $m$ such that $\sum_{j=1}^{m} M_j \leq n$, while $\mu_{jw}(n) = \mu_{wj}(n) + 1$, for a sequence $\{M_i\}$ of independent and identically distributed cluster sizes, independent of the spatio–temporal sequence $\{(R_i, T_i)\}$.

The waiting-jump and jump-waiting schemes may lead to different relaxation patterns. The result depends on the cluster-size properties. For finite-mean-value cluster sizes both scenarios provide the same result as the classical decoupled CTRW models. To obtain a general class of the two-power-law relaxation responses one should apply the clustering procedure characterized by the cluster sizes obeying a heavy-tailed distribution with the power-law exponent $0 < \gamma < 1$. In such a case the resulting diffusion front is modified by coupling between jumps and inter-jump times. Moreover, the waiting-jump and jump-waiting schemes lead to different relaxation responses [12].

For instance, let us take into account the case of heavy-tailed distributed waiting times for which

$$\Pr(T_i \geq t) \sim \left(\frac{t}{\tau_0}\right)^{-\alpha} \quad \text{as} \quad t \to \infty \,, \tag{6}$$

for some $0 < \alpha < 1, \tau_0 > 0$, and symmetric jumps $R_i$ with finite-mean-square length $\langle R_i^2 \rangle = \sigma^2 > 0$, independent of $T_i$. Then, if the cluster sizes have finite mean value, for both waiting-jump and jump-waiting schemes we obtain

$$\widetilde{R}(t) \stackrel{\mathrm{d}}{=} (At)^{\alpha/2}\, \mathcal{F}_\alpha \,, \tag{7}$$

where symbol "$\stackrel{\mathrm{d}}{=}$" denotes equal distributions, $A = \sigma^{2/\alpha}/\tau_0$, and $\mathcal{F}_\alpha$ is a fractional stable random variable, distributed as a mixture of completely asymmetric $\alpha$-stable law with standard Gaussian distribution[1]. The diffusion front (7) yields the Mittag–Leffler relaxation function

$$\Phi_{\mathrm{ML}}(t) = E_\alpha\left(-(\omega_p t)^\alpha\right) \,, \tag{8}$$

where $E_\alpha(x)$ is the Mittag–Leffler function [5, 10, 15] and $\omega_p = A|k|^{2/\alpha}$ denotes a positive, characteristic material constant. For this Mittag–Leffler

[1] Namely, $\mathcal{F}_\alpha \stackrel{\mathrm{d}}{=} \mathcal{S}_\alpha^{-\alpha/2}\mathcal{G}$, where $\mathcal{S}_\alpha$ is distributed according to the completely asymmetric Lévy-stable law with the index of stability $\alpha$, and $\mathcal{G}$ is a standard Gaussian random variable independent of $\mathcal{S}_\alpha$.

time-domain relaxation pattern, the corresponding frequency-domain response $\varepsilon(\omega)$ takes the CC form [10], which exhibits the power-law property (1) with $m = 1 - n = \alpha$.

On the other hand, if the cluster sizes have a heavy-tailed distribution with the power-law exponent $0 < \gamma < 1$, the waiting-jump scenario leads to

$$\widetilde{R}_{wj}(t) \stackrel{\mathrm{d}}{=} (At)^{\alpha/2}\, \mathcal{F}_\alpha \mathcal{B}_\gamma^{1/2}\,, \tag{9}$$

where $\mathcal{B}_\gamma$ is a generalized arcsine random variable[2] independent of the fractional stable random variable $\mathcal{F}_\alpha$, and $A$ is defined as in (7). However, for the jump-waiting scheme we have:

$$\widetilde{R}_{jw}(t) \stackrel{\mathrm{d}}{=} (At)^{\alpha/2}\, \mathcal{F}_\alpha \mathcal{B}_\gamma^{-1/2}\,. \tag{10}$$

To obtain diffusion fronts (7), (10), and (9), the scaling function has to be of the form $f(c) = (\Gamma(1-\alpha)c^{-\alpha})^{1/2}$, where $\Gamma(\cdot)$ is the gamma function.

For both cases the corresponding relaxation functions are generalizations of the Mittag–Leffler relaxation function (8). In the case of the waiting-jump diffusion front (9) we obtain the generalized Mittag–Leffler (GML) relaxation function [6]

$$\Phi_{wj}(t) = \Phi_{\mathrm{GML}}(t) = \int\limits_0^\infty E_\alpha\left(-(\omega_p t)^\alpha x\right) h_\gamma^{wj}(x)dx \tag{11}$$

with $h_\gamma^{wj}(x) = (\Gamma(\gamma)\Gamma(1-\gamma))^{-1} x^{\gamma-1}(1-x)^{-\gamma}$ for $0<x<1$, and 0 otherwise. In this scenario the corresponding frequency-domain response cannot be expressed in an analytical form. Nevertheless, the power-law exponents in (1) and the relationship between them can be derived by means of Tauberian theorems [6]. We get the following: $n = 1-\alpha$ and $m = \alpha\gamma < 1-n$, which fit the less typical (non-Havriliak–Negami) relaxation behavior, see Fig. 3.

The jump-waiting diffusion front (10) leads to

$$\Phi_{jw}(t) = \Phi_{\mathrm{HN}}(t) = \int\limits_0^\infty E_\alpha\left(-(\omega_p t)^\alpha x\right) h_\gamma^{jw}(x)dx \tag{12}$$

with $h_\gamma^{jw}(x) = (\Gamma(\gamma)\Gamma(1-\gamma))^{-1} x^{-1}(x-1)^{-\gamma}$ for $x > 1$, and 0 otherwise. (Notice that $h_\gamma^{jw}(x) = x^{-2} h_\gamma^{wj}\left(x^{-1}\right)$.) In this scenario the corresponding frequency domain response takes the form of the HN function (2) yielding the power-law property (1) with exponents $n = 1 - \alpha\gamma$ and $m = \alpha > 1 - n$, characteristic for the typical relaxation behavior.

[2] Generalized arcsine distribution with parameter $\gamma$ is just a beta distribution with parameters $\gamma$ and $1-\gamma$, $0 < \gamma < 1$.

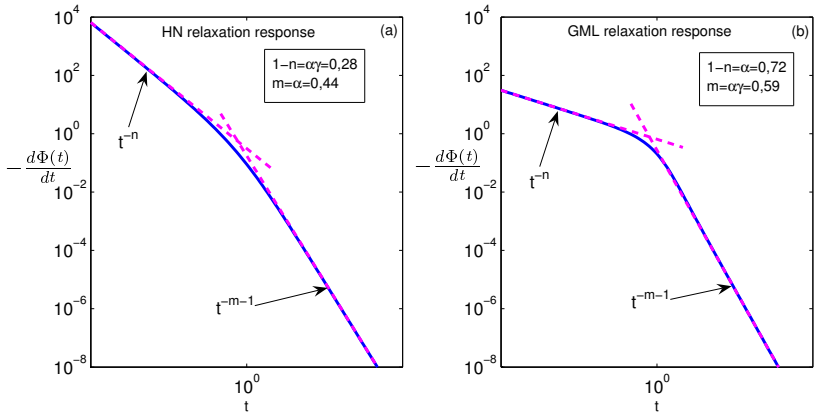


Fig. 3. Sample time-domain representation of the Havriliak–Negami and the generalized Mittag–Leffler responses. Values of the power-law exponents as for the experimental data presented in Fig. 2.

Notice that for $0 < \alpha, \gamma < 1$ we can represent the obtained relaxation functions in the form of a weighted average of an exponential decay $e^{-bt}$ with respect to the distribution of the effective relaxation rate $b$. Namely, we have $\Phi_{\mathrm{GML}}(t) = \int_0^\infty e^{-bt} g_{\mathrm{GML}}(b) db$ for

$$g_{\mathrm{GML}}(b) = \begin{cases} \dfrac{\sin(\gamma\psi(b))(\pi b)^{-1}}{((b/\omega_p)^{-2\alpha} + 2(b/\omega_p)^{-\alpha}\cos(\pi\alpha) + 1)^{\gamma/2}} & \text{for} \quad b > 0\,, \\ 0 & \text{for} \quad b \leq 0\,, \end{cases}$$

where $\psi(b) = \dfrac{\pi}{2} - \arctan\left(\dfrac{(b/\omega_p)^{\alpha} + \cos(\pi\alpha)}{\sin(\pi\alpha)}\right)$. Similarly, we can obtain $\Phi_{\mathrm{HN}}(t) = \int_0^\infty e^{-bt} g_{\mathrm{HN}}(b) db$ for

$$g_{\mathrm{HN}}(b) = \begin{cases} \dfrac{1}{\pi b}\,\dfrac{\sin(\gamma\psi(b))}{((b/\omega_p)^{2\alpha} + 2(b/\omega_p)^{\alpha}\cos(\pi\alpha) + 1)^{\gamma/2}} & \text{for} \quad b > 0\,, \\ 0 & \text{for} \quad b \leq 0\,, \end{cases}$$

where $\psi(b) = \dfrac{\pi}{2} - \arctan\left(\dfrac{(b/\omega_p)^{-\alpha} + \cos(\pi\alpha)}{\sin(\pi\alpha)}\right)$. At this point we have to stress that such a representation, following the most natural attempt to non-exponential relaxation [1], is not possible for the HN relaxation function with $\gamma > 1$.

Let us add that considering jumps $R_i$ satisfying another properties than finite mean-square length (*e.g.* heavy-tailed distributed jumps) one obtains the same relaxation patterns [4, 16]. The assumed type of the jump distribution influences the characteristic material constant $\omega_p$ only.

## 3. Conclusions

We have shown that the clustered-jump CTRW underlies a general class of the two-power-law relaxation patterns experimentally observed in various types of complex materials. The proposed model results from the stochastic generalization of the renormalization-group transformation idea applied to the CTRW. The resulting new type of the coupled-memory walk brings into limelight the stochastic origins of the low- and high-frequency power laws and clarifies the mutual relation between the power-law exponents. It gives waiting-jump and jump-waiting diffusion schemes which may lead to different relaxation processes depending on the cluster-size properties. If the distribution of cluster sizes possesses a heavy tail then the waiting-jumps scenario leads to the generalized Mittag–Leffler relaxation function, whereas the jump-waiting scheme results in the Hariliak–Negami function. The finite-mean-value clusters do not lead beyond the well-known subdiffusion scenario underlying the CC relaxation.

The work of A.J. and J.T. was partially supported by the project number POIG.01.03.01-02-002/08.

REFERENCES

[1] A.K. Jonscher, *Dielectric Relaxation in Solids*, Chelsea Dielectrics Press, London 1983.
[2] S. Havriliak Jr., S.J. Havriliak, *J. Non-Cryst. Solids* **172–174**, 297 (1994).
[3] Y.P. Kalmykov, W.T. Coffey, D.S.F. Crothers, S.V. Titov, *Phys. Rev.* **E70**, 041103 (2004).
[4] K. Weron, A. Jurlewicz, M. Magdziarz, *Acta Phys. Pol. B* **36**, 1855 (2005).
[5] R. Metzler, J. Klafter, *Phys. Rep.* **339**, 1 (2000).
[6] A. Jurlewicz, K. Weron, M. Teuerle, *Phys. Rev.* **E78**, 011103 (2008).
[7] M. Włodarska, G. Bak, B. Mossety-Leszczak, H. Galina, T. Pakuła, *J. Non. Cryst. Solids* **353**, 4371 (2007).
[8] C. Leighton, I. Terry, P. Becla, *Phys. Rev.* **B56**, 6689 (1996).
[9] M. Magdziarz, K. Weron, *Physica A* **367**, 1 (2006).
[10] K. Weron, M. Kotulski, *Physica A* **232**, 180 (1996).
[11] E. Gudowska-Nowak, K. Bochenek, A. Jurlewicz, K. Weron, *Phys. Rev.* **E72**, 061101 (2005).
[12] A. Jurlewicz, *Diss. Math.* **431**, 1 (2005).
[13] M.O. Vlad, *Phys. Rev.* **A45**, 3600 (1992).
[14] M.O. Vlad, *Phys. Rev.* **E51**, 3104 (1995).
[15] V.M. Zolotarev, *One-dimensional Stable Distributions*, American Mathematical Society, Providence 1986.
[16] A. Jurlewicz, K. Weron, *Acta Phys. Pol. B* **39**, 1055 (2008).